Published in final edited form as:
Cell Stem Cell. 2012 May 4; 10(5): 520–530. doi:10.1016/j.stem.2012.04.007.

CDC42 ACTIVITY REGULATES HEMATOPOIETIC STEM CELL AGING AND REJUVENATION

Maria Carolina Florian[1], **Karin Dörr**[1], **Anja Niebel**[1], **Deidre Daria**[1], **Hubert Schrezenmeier**[2], **Markus Rojewski**[2], **Marie-Dominique Filippi**[3], **Anja Hasenberg**[4], **Matthias Gunzer**[4], **Karin Scharffetter-Kochanek**[1], **Yi Zheng**[3], and **Hartmut Geiger**[1,3]

[1]Department of Dermatology and Allergic Diseases, University of Ulm, Ulm, Germany

[2]Institute for Clinical Transfusion Medicine and Immunogenetics Ulm, University of Ulm, Ulm, Germany

[3]Division of Experimental Hematology and Cancer Biology, Cincinnati Children's Hospital Medical Center and University of Cincinnati, Cincinnati, OH, USA

[4]Universität Duisburg/Essen, University Hospital, Institute of Experimental Immunology and Imaging, Essen, Germany

SUMMARY

The functional decline in hematopoietic function seen during aging involves a progressive reduction in the immune response and an increased incidence of myeloid malignancy, and has been linked to aging of hematopoietic stem cells (HSCs). The molecular mechanisms underlying HSC aging remain unclear. Here we demonstrate that elevated activity of the small RhoGTPase Cdc42 in aged HSCs is causally linked to HSC aging and correlates with a loss of polarity in aged HSCs. Pharmacological inhibition of Cdc42 activity functionally rejuvenates aged HSCs, increases the percentage of polarized cells in an aged HSC population, and restores the level and spatial distribution of histone H4 lysine 16 acetylation to a similar status as seen in young HSCs. Our data therefore suggest a mechanistic role for Cdc42 activity in HSC biology and epigenetic regulation, and identify Cdc42 activity as a pharmacological target for ameliorating stem cell aging.

Correspondence: Hartmut Geiger, Aging Research, KFO142, Department of Dermatology and Allergic Diseases, Ulm University, 89091 Ulm, Germany; hartmut.geiger@uni-ulm.de, Phone: 513-636-1338 or +49 731 500 57650; Fax: 513-636-3768 or +49 731 500 57652.

AUTHOR CONTRIBUTIONS

M.C.F. and H.G. designed and interpreted experiments and wrote the manuscript. M.C.F. performed and analyzed experiments. H.G. helped in performing transplantation experiments. K.D. and D.D. assisted in transplantation procedures and K.D, D.D. M.R. and H.S supported in cell sorting and flow analysis procedures. A.N. assisted in transplantation procedures and supported the Cdc42GAP mouse colony. A.H. and M.G. supported experiments with respect to intra-vital imaging. M-D.F., K.S-K. and Y.Z. assisted in designing and interpreting experiments.

CONFLICT OF INTEREST

The authors declare no competing financial interests.

INTRODUCTION

In the hematopoietic system, aging is driven by both intrinsic and extrinsic factors (Chambers and Goodell, 2007; Dorshkind and Swain, 2009; Geiger et al., 2005; Geiger and Van Zant, 2002; Ju et al., 2007; Morrison et al., 1996; Rando, 2006; Rossi et al., 2005) and manifests as decreased immune response (Linton and Dorshkind, 2004), increased myelogenous disease (Kiss et al., 2007; Signer et al., 2007), late-onset anemia (Beghe et al., 2004) and reduced regenerative capacity (Ergen and Goodell, 2009). Multiple studies and our own data demonstrate that the aged murine hematopoietic system is impaired in supporting peripheral blood (PB) leukocyte numbers (Figure S1A), erythropoiesis (Figure S1B–C), B-lymphoid and T-lymphoid cells (Figure S1D), while the number of myeloid cells is increased (Figure S1D). Changes in the total number of primitive hematopoietic cells with age are strain-dependent (Kamminga et al., 2005) and at least in part intrinsic to HSCs. For example in C57BL/6 mice, early hematopoietic progenitor cells ($Lineage^{neg}c\text{-}Kit^{+}Sca\text{-}1^{+}$ or LSK) and long-term repopulating-HSC ($LSKCD34^{low/-}Flk\text{-}2^{-}$, LT-HSC) numbers increase with age (Figure S1E–F), while lymphoid-primed multipotent progenitors (LMPPs, $LSKCD34^{+}Flk\text{-}2^{+}$(Adolfsson et al., 2005)) decrease (Figure S1F). Independent of the strain, aged HSCs show reduced self-renewal activity determined in serial transplant/engraftment assays (Janzen et al., 2006; Rossi et al., 2005) and exhibit a 2-fold reduced ability to home to the bone marrow (BM) (Liang et al., 2005). Moreover, aged LSKs are less efficient in their ability to adhere to stroma cells and exhibit significantly elevated cell protrusion activity *in vivo* (Geiger et al., 2007; Kohler et al., 2009; Xing et al., 2006). Thus, a defined set of cell-intrinsic phenotypic and functional parameters separate young from aged HSCs. Due to the cell intrinsic component of HSC aging – as aged HSCs present with most of these phenotypes also when exposed to a young microenvironment – one refers to young HSCs and aged HSCs when speaking of HSCs from young and aged animals (Geiger and Rudolph, 2009).

Cdc42 belongs to the family of small Rho-GTPase and cycles between an active (GTP-bound) and an inactive (GDP-bound) state. Cdc42 is known to regulate actin and tubulin organization, cell-cell and cell-extracellular matrix adhesion and cell-polarity in distinct cell types (Cau and Hall, 2005; Etienne-Manneville, 2004; Florian and Geiger, 2010; Sinha and Yang, 2008). Our previous and current studies demonstrate that Cdc42 activity is significantly increased both in primitive hematopoietic cells (Figure S1G) as well as in other tissues of aged mice compared to cells from young animals (Xing et al., 2006). Based on this observation we hypothesize that the aging-associated increased Cdc42 activity in HSCs may causatively regulate cell intrinsic aging of HSCs (Geiger et al., 2007; Kohler et al., 2009).

RESULTS

Constitutively increased Cdc42 activity results in aging-like phenotypes in young HSCs

To test the role of Cdc42 activity in cell-intrinsic aging of HSCs, we determined whether constitutively increased Cdc42 activity in young HSCs by genetic means is sufficient to resemble aging-like phenotypes in HSCs, using as a model HSCs deficient for the p50RhoGAP protein ($Cdc42GAP^{-/-}$ mice). This RhoGAP protein is a highly selective negative regulator of Cdc42-activity (Barfod et al., 1993), and therefore $Cdc42GAP^{-/-}$ mice present with a gain-of-activity specific for Cdc42 in all tissues (Wang et al., 2007), including primitive hematopoietic cells (Figures S1I). Supporting our hypothesis, $Cdc42GAP^{-/-}$ mice present with premature aging-like phenotypes in multiple tissues and cell types (Wang et al., 2007). As for the hematopoietic system, a significant increase in myeloid cell frequency and a decrease in T cell frequency in PB was detected in young $Cdc42GAP^{-/-}$ mice as well as an overall decrease of B-cell frequency and an increase in myeloid cell frequency in BM, which are phenotypes consistent with aging in hematopoiesis (Figure S1J). To determine the

functional status of Cdc42GAP$^{-/-}$ HSC, competitive serial transplant assays were performed (Figure 1A), which are regarded as a gold standard for determining stem cell intrinsic parameters of HSC aging (Chambers and Goodell, 2007; Rossi et al., 2005; Rossi et al., 2008). Results demonstrated that young Cdc42GAP$^{-/-}$ HSCs resemble aged HSCs and were significantly distinct from young control Cdc42GAP$^{+/+}$ HSCs with respect to their repopulation ability (Figure 1B), contribution to the B-cell lineage and contribution to the myeloid cell lineage in PB (Figure 1C–D) as well as in BM (Figure S1M–N) in both primary and secondary recipients. Furthermore, young Cdc42GAP$^{-/-}$ cells, similarly to aged, contributed significantly more to the pool of LT-HSCs compared to young Cdc42GAP$^{+/+}$ controls both in primary and in secondary recipients (Figure 1E–G). There was also a significant decrease in the contribution of aged and Cdc42GAP$^{-/-}$ HSCs to LMPPs in secondary recipients compared to young Cdc42GAP$^{+/+}$ cells (Figure 1G). Thus, chronologically young Cdc42GAP$^{-/-}$ HSCs are functionally similar to chronologically aged HSCs in competitive transplantation assays. These data imply a mechanistic role for intrinsically elevated Cdc42 activity in chronologically aged HSCs for phenotypic and functional changes associated with aged HSCs.

Increased Cdc42 activity in HSCs correlates with a de-polarized phenotype in LT-HSCs

In *D. melanogaster*, the age-associated loss of germ-line stem cell function correlates with loss of cell polarity (Cheng et al., 2008). We recently reported a reduction in the frequency of cells with a polar distribution of microtubules among aged early hematopoietic progenitor cells (LSK cells) (Kohler et al., 2009). Cdc42 activity has been implicated in the regulation of polarity in fibroblasts and epithelial cells (Cau and Hall, 2005; Iden and Collard, 2008) and in the maintenance of polarity and stemness in neuronal stem cells (Cappello et al., 2006). Based on these observations we next investigated whether the polarity status of LT-HSCs changes upon aging, and whether Cdc42 activity might be causally involved in regulating such changes. To test this we initially determined the localization of Cdc42, which in itself is a cell polarity marker (Etienne-Manneville, 2004) and tubulin in LT-HSCs in single-cell immunofluorescence (IF) analyses performed on LT-HSCs. Interestingly, in the majority of young LT-HSCs, Cdc42 and tubulin were asymmetrically distributed and were found at the same location inside the cell (Figure 2A and C, Figure S2A and C and movie S1). This highly asymmetric localization of Cdc42 and tubulin did not correlate with the side of the cell bound to the substrate nor with an uneven distribution of the whole cytoplasm, as for example F-actin always showed a cortical and unpolarized distribution (Figure S2E–F and movie S2). The asymmetry was oriented along the *xy* plane on one the side of the nucleus where also the centrosome was localized (Figure 2A, panels ix–xii and movie S1). Therefore, in young LT-HSCs, Cdc42 and the microtubules were highly concentrated in the immediate pericentriolar zone and in the cytoplasmatic space along the nucleus/centrosome/cell membrane axis (Figure 2A and D, movie S1). In contrast, Cdc42 and tubulin were distributed throughout the cell body in an unpolarized fashion in aged LT-HSCs (Figure 2B–C, Figure S2B, D and F and movie S3) and the centrosome was mostly found in the middle of the cell, oriented perpendicularly to the nucleus along the *z*-axis (Figure 2B panels ix–xi, Figure 2D and movie S3). Similar results (young HSCs polar, aged HSCs apolar) were also obtained by analyzing additional established cell polarity markers like Crumbs3 (Figure S2G and I–J) and Dgl (Figure S2G and K). Par6 (Figure S2G and L) and the aPKCζ (Figure S2G) did not follow this pattern, in agreement with recently published data (Sengupta et al., 2011). Interestingly, the difference in polarity among young and aged primitive hematopoietic cells is specific to LT-HSCs as for example we did not observed a difference between young and aged ST-HSCs (Figure S2H) and it is not correlated to the cycle status, as young and aged LT-HSC show very similar cell cycle parameter profiles (Figure S1H and also (Chambers et al., 2007; Rossi et al., 2007; Silva and Conboy, 2008; Sudo et al., 2000)). In summary, chronologically young HSCs present with a

polarity phenotype similar to the one previously described for memory T-cells (Chang et al., 2007; Ludford-Menting et al., 2005) - which is lost upon aging of LT-HSCs. Recently CD150 expression was described as a marker for functionally distinct subpopulations within the pool of LT-HSCs (Beerman et al., 2010). The polarity phenotype identifying phenotypically different type of LT-HSCs (polar vs. apolar) might thus constitute another surrogate marker for the distinct cell subsets stained by CD150 expression. The frequency of young LT-HSCs polarized for Cdc42 and tubulin though was independent of the expression of CD150 on LT-HSCs (Figure S2M–N).

Consistent with a critical role of elevated Cdc42 activity in age-associated phenotypes like apolarity, IF staining revealed that the majority of chronologically young Cdc42GAP$^{-/-}$ LT-HSCs, which functionally resemble aged LT-HSCs, were apolar with respect to Cdc42 and tubulin distribution (Figure 2E–F). In addition, consistently with our observations comparing chronologically young and aged LT-HSCs (Figure S1H), young Cdc42GAP$^{+/+}$, Cdc42GAP$^{-/-}$ and aged LT-HSCs present with a similar cell cycle and apoptosis profile (Figure S1K–L), strongly implying that differences in polarity are independent of these parameters. These data thus identify Cdc42 as a novel polarity protein in LT-HSCs showing distinct polarity phenotypes in young and aged LT-HSCs and supporting at a role for Cdc42 activity specifically in the regulation of LT-HSC polarity.

Pharmacological reduction of Cdc42 activity rejuvenates aged LT-HSCs function and restores the level and the spatial distribution of histone H4 lysine 16 acetylation

Our data imply that the aging-associated increase in Cdc42 activity might be a stem-cell intrinsic molecular mechanism resulting in both apolarity and impaired function of LT-HSCs with age. We consequently reasoned that inhibiting Cdc42 activity in aged LT-HSCs to the level in young LT-HSCs by pharmacological means might be a possible approach to at least in part revert apolarity as well as the impaired function of aged LT-HSCs. To exclude stem cell extrinsic effects and focus on cell intrinsic mechansims, LT-HSCs from aged mice were treated *in vitro* with a selective Cdc42 activity inhibitor (Sakamori et al., 2012) (newly termed CASIN, referred to in (Peterson et al., 2006) as Pirl1-related compound 2) *(for structure and specificity of CASIN see accompanying data by Liu et al. part of a manuscript currently under revision)*. Treatment with CASIN (5μM) reduced the elevated level of active Cdc42 observed in aged primitive hematopoietic cells to the level observed in young cells (Figure 3A–B). CASIN treatment did not alter cell cycle status or apoptosis in aged LT-HSCs (Figure S3A–C). In response to treatment with CASIN, LT-HSCs from aged mice showed a dose-dependent increase in the percentage of polarized cells, becoming progressively indistinguishable from young cells (Figure 3C–D). These data demonstrate that elevated Cdc42-GTP levels in aged LT-HSCs cell-intrinsically regulate both Cdc42 and tubulin distribution and that the apolar distribution of these proteins can be reverted to a polar one by decreasing Cdc42 activity. Thus, CASIN treatment reverted aged LT-HSCs to young HSCs with respect to the polarity phenotype.

We next determined whether inhibition of Cdc42 activity in aged LT-HSCs via CASIN treatment could revert at least in part the altered function of aged LT-HSCs to become functionally younger. Although CASIN acts transiently on Cdc42 activity, surprisingly the increase in the percentage of polar cells among aged LT-HSCs induced by CASIN *in vitro* remained stable for at least up to 6 hours after CASIN withdrawal (Figure S3D–E). This result implies a kind of “polarity memory” upon transient reduction of Cdc42 activity in aged LT-HSCs, which might allow for continuation of the new polar phenotype and the associated function(s) upon transplantation into recipient animals. Therefore, 200 aged LT-HSCs treated with 5μM CASIN overnight were competitively serially transplanted into young recipients and compared to transplants with young and aged untreated LT-HSCs (Figure 4A). In primary recipients, overall donor engraftment after 8, 16 and 24 weeks was

similar in aged control and aged CASIN treated LT-HSCs (Figure 4B), but remarkably, CASIN treatment of aged LT-HSCs resulted in an increase in contribution to the B-cell compartment in PB and a reduced contribution to the myeloid lineage (Figure 4D). In addition, CASIN treatment increased the contribution to LSK and common lymphoid progenitor (CLP) populations to a level indistinguishable from young LT-HSCs (Figure S4A). The frequency of donor-derived LT-HSCs among donor-derived LSKs was, as anticipated, doubled in aged control recipients, while upon CASIN treatment this frequency was significantly reduced (Figure 4F). In addition, upon secondary transplant CASIN treated LT-HSCs presented with an elevated overall regenerative capacity compared to aged LT-HSCs, as indicated by increased and stable chimerism in PB (Figure 4C). Moreover, upon secondary transplant CASIN treated aged LT-HSCs proved to be indistinguishable from young LT-HSCs with respect to B-cell and myeloid engraftment in PB and BM (Figure 4E and Figure S4B–C) and with respect to the contribution to the LT-HSC pool in BM (Figure 4G). Young CASIN treated LT-HSCs which were competitively transplanted in experiments alongside the aged control and aged CASIN treated LT-HSCs transplants did not show any relevant functional changes compared to young control LT-HSCs (Figure S4D–K), demonstrating that CASIN reverts specifically aging-related phenotypes of aged LT-HSCs.

Since aged hematopoietic stem cells exhibit a 2-fold reduced ability to home to the BM (Dykstra et al., 2011; Liang et al., 2005) and aged early hematopoietic progenitor cells localize more distantly from the endosteum compared to young cells (Kohler et al., 2009), we next investigated whether also these aging-associated phenotypes were rejuvenated by CASIN treatment. Homing of young, aged and aged CASIN treated LT-HSCs was determined in competitive short-term homing assays (Dykstra et al., 2011) (Figure S5A), while the distance of LT-HSCs from the endosteum was measured by intravital two-photon microscopy (Kohler et al., 2009). The data indicate that CASIN treated aged LT-HSC present with significantly improved homing to the BM and localize closer to the endosteum (Figure S5B–F) compared to aged control LT-HSCs.

Finally, the frequency of polar donor-derived LT-HSCs in recipients transplanted with aged, aged CASIN treated and young primary LT-HSCs was determined 24 weeks post transplantation. The data indicate that the percentage of donor-derived polar LT-HSCs in recipients transplanted with aged CASIN treated LT-HSC was similar to the frequency found in young controls and significantly increased, at least with respect to Cdc42 localization, compared to the frequency found in aged untreated controls (Figure 4H–I).

One explanation for the long-lasting “memory effect” on aged LT-HSCs upon transient reduction of Cdc42 activity observed in our experiments might be that reduction of Cdc42 activity to the level seen in young results in epigenetic marker changes in aged LT-HSCs, accordingly with a proposed role for epigenetic regulation of stem cell aging (Pollina and Brunet, 2011; Rando and Chang, 2012). Acetylation of histones is a prevalent epigenetic chromatin modification in eukaryotes. Activated Cdc42 was reported to specifically alter acetylation of histone H4 in 3T3 cells (Alberts et al., 1998), and histone H4 acetylation has been shown to be mitotically stable and inheritable during development (Cavalli and Paro, 1999). On histone H4, lysine 16 is the most common site of acetylation, and controls chromatin structures as well interactions between non-histone proteins and chromatin fibers, while it is unique as it is the only lysine residue among N-terminal tails of all histones targeted by the Sir2 (or class III) family of HDACs (Vaquero et al., 2007). Histone H4 lysine 16 acetylation (AcH4K16) has been implicated in regulating yeast replicative aging (Dang et al., 2009), and AcH4K16 levels were found to be reduced in multiple tissue of aged mice (Krishnan et al., 2011).

Consequently, we investigated whether elevated Cdc42 activity might affect histone H4 acetylation levels as well as specifically AcH4K16 patterns in primitive hematopoietic cells including LT-HSCs. Our data demonstrate that young LT-HSCs express higher levels of AcH4K16 compared to young ST-HSCs and LMPPs (Figure 5A and D) in agreement with previous reports (Chung et al., 2009). Aged LT-HSCs present with an overall decreased level of AcH4K16 compared to young LT-HSCs, but still show higher levels of AcH4K16 compared to aged ST-HSCs and LMPPs (Figure 5A and D). Moreover, aged LT-HSC only present with two distinct subpopulations expressing low and high AcH4K16 levels (Figure 5A), which are not found in young LT-HSCs. Young LT-HSCs are almost exclusively AcH4K16^{high} cells while 34% of aged LT-HSCs present with a low AcH4K16 expression level. CASIN treatment induces a sharp decrease of the frequency of AcH4K16^{low} aged LT-HSCs while increasing the frequency of AcH4K16^{high} cells (Figure 5A–C). This effect of CASIN on AcH4K16 (Figure 5A–D) was specific to LT-HSCs (no effect on ST-HSCs and LMPPs), age specific (young CASIN treated LT-HSCs did not display any significant modification) and specific to acetylation of lysine 16 on histone H4 (the total level of acetylation on histone H4 was not altered, Figure 5E). Most interestingly, we observed that AcH4K16 localization within the nucleus of young LT-HSCs was polarized and opposite of the cytoplasmatic tubulin pole, while the great majority of aged LT-HSCs nuclei was apolar for AcH4K16 localization (Figure 5F–H and movies S4–5). Strikingly, CASIN treatment of aged LT-HSCs increased the frequency of aged LT-HSCs with a polar localization of AcH4K16 to a level similar to that found in young LT-HSCs (Figure 5F–H). Thus treatment of aged LT-HSCs with CASIN restores the level and the spatial distribution of AcH4K16 to the level seen in young LT-HSCs consistently with a previous suggested loss of epigenetic regulation in aged HSCs (Chambers et al., 2007; Pollina and Brunet, 2011). Importantly, our data does not exclude that inhibition of Cdc42 activity in aged LT-HSCs might also alter additional epigenetic marks like histone methylation patterns.

In summary, these data identify elevated Cdc42 activity as key modulator of a molecular pathway driving intrinsic mechanisms of stem cell aging. Furthermore, these results demonstrate that lowering Cdc42 activity by CASIN treatment rejuvenates aged LT-HSCs with respect to function (lineage skewing, regenerative capacity and homing) as well as phenotypic (polarity) and epigenetic (AcH4K16, both level of acetylation and localization within the nucleus) parameters.

DISCUSSION

Until recently, there was a broad consensus that the phenotype of aged HSCs is fixed and dominated by cell-intrinsic regulatory mechanisms that could not be reverted by therapeutic intervention. This paradigm recently started to shift (Rando and Chang, 2012), as it was demonstrated that impaired contribution to PB upon transplantation of aged HSCs could be ameliorated by either antioxidative therapy or rapamycin treatment (Chen et al., 2009; Ito et al., 2006). Our data significantly extend these observations as we demonstrate a critical mechanistic role of Cdc42 activity in HSC aging and identify it as a target to pharmacologically rejuvenate stem cell intrinsic age-associated phenotypes of LT-HSCs. Since also the differences in polarity between young and aged LT-HSCs with respect to Cdc42, tubulin and AcH4K16 are regulated by Cdc42 activity, these data further support a novel concept in which aging-associated changes in LT-HSC self-renewal and differentiation are possibly regulated by changes in stem cell polarity. Our data further identify a role for Cdc42 activity in regulating epigenetic modifications in LT-HSCs as well as polarity of epigenetic markers (epi-polarity) and the loss of this polarity upon aging as a novel concept in hematopoietic stem cell biology. Interestingly, a recent report described a prominent role for epigenetic modifications in transgenerational and thus long-term memory associated longevity in *C.elegans* (Greer et al., 2011). Furthermore, genome-wide

association studies have recently identified a positive correlation between *Cdc42* expression in human white blood cells and increased morbidity and aging (Kerber et al., 2009), while elevated Cdc42 activity was found in multiple tissues of aged mice, likely implying a role for the Cdc42-polarity pathway in aging not only of LT-HSCs.

EXPERIMENTAL PROCEDURES

Serial Competitive Transplantation

BM cells (10^6) from 4–6-week-old Cdc42GAP$^{+/+}$ and Cdc42GAP$^{-/-}$ mice and aged (20- to 26-month-old) C57BL/6 mice (donors, Ly5.2$^+$) were mixed with 10^6 BM cells from young (2–4-month-old) BoyJ competitor mice (Ly5.1$^+$) and injected into the retro-orbital sinus of irradiated BoyJ recipient mice (Ly5.1$^+$) in 200 μl in PBS. Primary transplanted mice were sacrificed after 20 weeks and 2×10^6 BM cells from each recipient mouse were injected into a secondary pre-conditioned recipient BoyJ mouse. Serial BM transplantation experiments were repeated three times with a cohort of 4 to 5 recipient mice per donor. For competitive LT-HSC transplantation, young (2–4-month-old) and aged (20–26-month-old) C57BL/6 mice (Ly5.2$^+$) were used as donors. 200 LT-HSCs were sorted into 96 multi-well plates and cultured (either in suspension or adherent to fibronectin) for 16hrs in HBSS+10%FBS ±CASIN (5μM) in a water-jacketed incubator at 37°C, 5%CO_2, 3%O_2. Stem cells were then mixed with 3×10^5 BM cells from young (2–4-month-old) BoyJ competitor mice (Ly5.1$^+$) and then transplanted into BoyJ recipient mice (Ly5.1$^+$). PB chimerism was determined by FACS analysis every 8 weeks. 24 weeks post primary transplants, 2×10^6 BM cells from an individual primary recipient mouse were injected into an individual secondary pre-conditioned recipient BoyJ mouse. Experiment was performed three times with LT-HSCs cultured in suspension and two times with LT-HSCs cultured on a fibronectin-coated substrate without any difference in experimental outcome. Primary transplanted mice were regarded engrafted when PB chimerism was higher or equal to 1.0% and contribution was detected in all lineages. Secondary transplanted mice were regarded as engrafted when PB chimerism was higher or equal to 0.5% and contribution was detected in all lineages.

Flow cytometry and cell sorting

PB and BM cell immunostaining was performed according to standard procedures and samples were analyzed on a LSRII flow cytometer (BD Biosciences). Lineage FACS analysis data are plotted as the percentage of B220$^+$, CD3$^+$ and Myeloid (Gr-1$^+$, Mac-1$^+$ and Gr-1$^+$Mac-1$^+$) cells among donor-derived Ly5.2$^+$ cells. As for early hematopoiesis analysis, mononuclear cells were isolated by low-density centrifugation (Histopaque 1083, Sigma) and stained with a cocktail of biotinylated lineage antibodies. After lineage depletion by magnetic separation (Dynalbeads, Invitrogen), cells were stained with anti-Sca-1 (clone D7) (eBioscience), anti-c-kit (clone 2B8) (eBioscience), anti-CD34 (clone RAM34) (eBioscience), anti-CD127 (clone A7R34) (eBioscience), anti-Flk-2 (clone A2F10) (eBioscience) and Streptavidin (eBioscience). Early hematopoiesis FACS analysis data were plotted as percentage of long-term hematopoietic stem cells (LT-HSCs, gated as LSK CD34$^{-/low}$Flk2$^-$), short-term hematopoietic stem cells (ST-HSCs, gated as LSK CD34$^+$Flk2$^-$) and lymphoid-primed multipotent progenitors (LMPPs, gated as LSK CD34$^+$Flk2$^+$) (Adolfsson et al., 2005) distribution among donor-derived LSKs (Lin^{neg}c-kit$^+$sca-1$^+$ cells). LSK and common lymphoid progenitor cells (CLP, gated as Lin$^-$ c-Kit$^{+/low}$ Sca-1$^{+/low}$ IL7Rα$^+$) (Karsunky et al., 2008) were plotted as percentage among donor-derived Lin^{neg} cells. In order to isolate LT-HSCs, lineage depletion was performed to enrich for lineage negative cells. Lineage negative cells were then stained as aforementioned and sorted using a BD FACS Aria I or a BD FACS Aria III (BD Bioscience). For intracellular flow cytometric staining of AcH4 and AcH4K16, lineage depleted young and aged BM cells where incubated for 16 hrs with or without CASIN 5μM in IMDM+10%FBS

at 37°C, 5%CO_2, 3%O_2. At the end of the treatment, the samples were moved on ice and stained again with the cocktail of biotinylated lineage antibodies. After washing the samples were stained with anti-Sca-1 (clone D7) (eBioscience), anti-c-kit (clone 2B8) (eBioscience), anti-CD34 (clone RAM34) (eBioscience), anti-Flk-2 (clone A2F10) (eBioscience) and Streptavidin (eBioscience). At the end of the surface staining, cells were fixed and permeabilized with Cytofix/Cytoperm Solution (BD Biosciences) and incubated with 10% Donkey Serum (Sigma) in BD Perm/Wash Buffer (BD Biosciences) for 30 minutes. Primary and secondary antibodies incubations were performed at room temperature in BD Perm/Wash Buffer (BD Biosciences) for 1hr and 30 min respectively. The primary antibodies for acetylated histone H4 were obtained all by Upstate-Millipore (rabbit anti-acetyl-histone H4 Lys5, Lys8, Lys12 and Lys16). The secondary antibody is a donkey anti-rabbit DyLight649 (BioLegend).

Immunofluorescence staining

Freshly sorted LT-HSCs were seeded on fibronectin-coated glass coverslips in HBSS +10%FBS. CASIN (referred to in (Peterson et al., 2006) as Pirl1-related compound 2) was obtained from Chembridge Corporation, and purified to greater than 99% by high-performance liquid chromatography. After 16 hours of incubation at 37°C, 5%CO_2, 3%O_2, in growth factors-free medium cells were fixed with BD Cytofix Fixation Buffer (BD Biosciences). After fixation cells were gently washed with PBS, permeabilized with 0.2% Tryton X-100 (Sigma) in PBS for 20 minutes and blocked with 10% Donkey Serum (Sigma) for 30 minutes. Primary and secondary antibodies incubations were performed for 1hr at room temperature. Coverslips were mounted with ProLong Gold Antifade Reagent with or without DAPI (Invitrogen, Molecular Probes). The cells were coimmunostained with an anti-alpha tubulin antibody (Abcam, rat monoclonal ab6160) detected with an anti-rat AMCA-conjugated secondary antibody or an anti-rat DyLight488-conjugated antibody (Jackson ImmunoResearch), an anti-Cdc42 antibody (Millipore, rabbit polyclonal) or an anti-AcH4K16 antibody (Upstate-Millipore, rabbit polyclonal) detected with an anti-rabbit DyLight549-conjugated antibody (Jackson ImmunoResearch) and/or an anti-Pericentrin-2 antibody (Santa Cruz Biotechnology, goat polyclonal) detected with an anti-goat AMCA-conjugated antibody (Jackson ImmunoResearch). Samples were imaged with an AxioObserver Z1 microscope (Zeiss) equipped with a 63X PH objective. Images were analyzed with AxioVision 4.6 software. Alternatively, samples were analyzed with an LSM710 confocal microscope (Zeiss) equipped with a 63X objective. Primary raw data were imported into the Volocity Software package (Version 6.0, Perkin Elmer) for further processing and conversion into 3-dimensional images. As for polarity scoring, the localization of each single stained protein was considered polarized when a clear asymmetric distribution was visible by drawing a line across the middle of the cell. A total of 50 to 100 LT-HSCs were singularly analyzed per sample. Data are plotted as percentage of the total number of cells scored per sample. Specificity of the anti-Cdc42 antibody in immunofluorescence was tested on LT-HSCs sorted from mice in which *cdc42* was targeted deleted specifically in the hematopoietic system (Mx1-Cre;$Cdc42^{flox/flox}$ mice (Yang et al., 2007)) (data not shown).

Competitive short-term homing assay and intravital two-photon microscopy

For competitive short-term homing assay (Dykstra et al., 2011), LT-HSCs were sorted from young and aged mice and incubated for 16hrs in HBSS+10%FBS±CASIN (5μM) in a water-jacketed incubator at 37°C, 5%CO_2, 3%O_2. After treatment, LT-HSCs were labelled with the cell tracker CFSE (Invitrogen-Molecular probes) or the cell tracker CMRA (Invitrogen-Molecular probes), washed and mixed to inject 5000 young+5000 aged LT-HSCs or 5000 aged+5000 aged CASIN treated LT-HSCs into each lethally irradiated young recipient mouse (figure S4L). After 16–18 hrs from the stem cell injection, recipient mice were

sacrificed and all BM cells were analyzed by flow cytometry to quantify relative frequency of $CFSE^+$ and $CMRA^+$ cells. A total of 6 recipient mice were injected per experiment (3 receiving 5000 $CFSE^+$ young LT-HSCs mixed with 5000 $CMRA^+$ aged LT-HSCs each and 3 receiving 5000 $CFSE^+$ aged CASIN treated LT-HSCs mixed with 5000 $CMRA^+$ aged LT-HSCs each) and the experiment was repeated twice. For intravital two-photon microscopy analysis, LT-HSCs were sorted, treated, labelled and mixed as aforementioned but injected into non-irradiated recipient young mice. A total of 4 recipient mice were injected per experiment (2 receiving 5000 $CFSE^+$ young LT-HSCs mixed with 5000 $CMRA^+$ aged LT-HSCs each and 2 receiving 5000 $CFSE^+$ aged CASIN treated LT-HSCs mixed with 5000 $CMRA^+$ aged LT-HSCs each). After 16–18 hrs from the stem cell injection, recipient mice were prepared for intravital microscopy as previously described (Kohler et al., 2009) using isofluran-based intubation narcosis. Briefly, the tibiae were exposed and part of the bone tissue was carefully removed with an electric drill (Dremel) to obtain a very thin (30–50 μm) remaining layer of bone tissue covering the BM cavity. This procedure was permanently controlled by stereomicroscopy. The bone tissue was identified due to its strong autofluorescence (CCD) under unfiltered light conditions or using its second-harmonic (SHG) signal (PMT). Animals were kept at 37°C in a PBS water bath while experiments were performed. For imaging, the area was scanned down to ~120μm depth (more than 12 cell layers) using an illumination wavelength of either 800 or 880 nm detecting CFSE (530nm) and CMRA (580nm) fluorescence, as well as unfiltered light or SHG (at 480nm emission). Primary raw data were imported into the Volocity Software package (Version 6.0, Perkin Elmer) for further processing and conversion into 3-dimensional images and for measurement of the distance between LT-HSCs and the endosteum.

HIGHLIGHTS

1. Constitutively increased Cdc42 activity results in aging of young HSCs
2. Elevated activity of Cdc42 correlates with a loss of cell polarity in aged HSCs
3. Inhibiting Cdc42 activity rejuvenates aged LT-HSCs function
4. Inhibiting Cdc42 activity restores the level and spatial distribution of AcH4K16

Supplementary Material

Refer to Web version on PubMed Central for supplementary material.

Acknowledgments

We thank Gary Van Zant, Jose A. Cancelas, Marnie A. Ryan and Hartmut Weiler for advice and critical reading of the manuscript. We thank Frank Kirchhoff and Dré van der Merwe for cell sorting support, Angelika Rück and the Institut für Lasertechnologien in der Medizin und Meßtechnik of Ulm University for support with confocal microscopy and the Tierforschungszentrum of the University of Ulm for supporting our animal work. This work was supported by grants from the Deutsche Forschungsgemeinschaft KFO 142, GE2063/1 and from the National Institute of Health, HL076604, DK077762 and AG040118 to H.G. and a “Bausteinprogramm” of the Department of Medicine Ulm to M.C.F.

REFERENCES

Adolfsson J, Mansson R, Buza-Vidas N, Hultquist A, Liuba K, Jensen CT, Bryder D, Yang L, Borge OJ, Thoren LA, et al. Identification of Flt3+ lympho-myeloid stem cells lacking erythro-megakaryocytic potential a revised road map for adult blood lineage commitment. Cell. 2005; 121:295–306. [PubMed: 15851035]

Alberts AS, Geneste O, Treisman R. Activation of SRF-regulated chromosomal templates by Rho-family GTPases requires a signal that also induces H4 hyperacetylation. Cell. 1998; 92:475–487. [PubMed: 9491889]

Barfod ET, Zheng Y, Kuang WJ, Hart MJ, Evans T, Cerione RA, Ashkenazi A. Cloning and expression of a human CDC42 GTPase-activating protein reveals a functional SH3-binding domain. J Biol Chem. 1993; 268:26059–26062. [PubMed: 8253717]

Beerman I, Bhattacharya D, Zandi S, Sigvardsson M, Weissman IL, Bryder D, Rossi DJ. Functionally distinct hematopoietic stem cells modulate hematopoietic lineage potential during aging by a mechanism of clonal expansion. Proc Natl Acad Sci U S A. 2010; 107:5465–5470. [PubMed: 20304793]

Beghe C, Wilson A, Ershler WB. Prevalence and outcomes of anemia in geriatrics: a systematic review of the literature. Am J Med. 2004; 116(Suppl 7A):3S–10S. [PubMed: 15050882]

Cappello S, Attardo A, Wu X, Iwasato T, Itohara S, Wilsch-Brauninger M, Eilken HM, Rieger MA, Schroeder TT, Huttner WB, et al. The Rho-GTPase cdc42 regulates neural progenitor fate at the apical surface. Nat Neurosci. 2006; 9:1099–1107. [PubMed: 16892058]

Cau J, Hall A. Cdc42 controls the polarity of the actin and microtubule cytoskeletons through two distinct signal transduction pathways. J Cell Sci. 2005; 118:2579–2587. [PubMed: 15928049]

Cavalli G, Paro R. Epigenetic inheritance of active chromatin after removal of the main transactivator. Science. 1999; 286:955–958. [PubMed: 10542150]

Chambers SM, Goodell MA. Hematopoietic stem cell aging: wrinkles in stem cell potential. Stem Cell Rev. 2007; 3:201–211. [PubMed: 17917133]

Chambers SM, Shaw CA, Gatza C, Fisk CJ, Donehower LA, Goodell MA. Aging hematopoietic stem cells decline in function and exhibit epigenetic dysregulation. PLoS Biol. 2007; 5:e201. [PubMed: 17676974]

Chang JT, Palanivel VR, Kinjyo I, Schambach F, Intlekofer AM, Banerjee A, Longworth SA, Vinup KE, Mrass P, Oliaro J, et al. Asymmetric T lymphocyte division in the initiation of adaptive immune responses. Science. 2007; 315:1687–1691. [PubMed: 17332376]

Chen C, Liu Y, Zheng P. mTOR regulation and therapeutic rejuvenation of aging hematopoietic stem cells. Sci Signal. 2009; 2:ra75. [PubMed: 19934433]

Cheng J, Turkel N, Hemati N, Fuller MT, Hunt AJ, Yamashita YM. Centrosome misorientation reduces stem cell division during ageing. Nature. 2008; 456:599–604. [PubMed: 18923395]

Chung YS, Kim HJ, Kim TM, Hong SH, Kwon KR, An S, Park JH, Lee S, Oh IH. Undifferentiated hematopoietic cells are characterized by a genome-wide undermethylation dip around the transcription start site and a hierarchical epigenetic plasticity. Blood. 2009; 114:4968–4978. [PubMed: 19752395]

Dang W, Steffen KK, Perry R, Dorsey JA, Johnson FB, Shilatifard A, Kaeberlein M, Kennedy BK, Berger SL. Histone H4 lysine 16 acetylation regulates cellular lifespan. Nature. 2009; 459:802–807. [PubMed: 19516333]

Dorshkind K, Swain S. Age-associated declines in immune system development and function: causes, consequences, and reversal. Curr Opin Immunol. 2009; 21:404–407. [PubMed: 19632102]

Dykstra B, Olthof S, Schreuder J, Ritsema M, de Haan G. Clonal analysis reveals multiple functional defects of aged murine hematopoietic stem cells. J Exp Med. 2011

Ergen AV, Goodell MA. Mechanisms of hematopoietic stem cell aging. Exp Gerontol. 2009

Etienne-Manneville S. Cdc42--the centre of polarity. J Cell Sci. 2004; 117:1291–1300. [PubMed: 15020669]

Florian MC, Geiger H. Concise review: polarity in stem cells, disease, and aging. Stem Cells. 2010; 28:1623–1629. [PubMed: 20641041]

Geiger H, Koehler A, Gunzer M. Stem cells, aging, niche, adhesion and Cdc42: a model for changes in cell-cell interactions and hematopoietic stem cell aging. Cell Cycle. 2007; 6:884–887. [PubMed: 17404508]

Geiger H, Rennebeck G, Van Zant G. Regulation of hematopoietic stem cell aging in vivo by a distinct genetic element. Proc Natl Acad Sci U S A. 2005; 102:5102–5107. [PubMed: 15788535]

Geiger H, Rudolph KL. Aging in the lympho-hematopoietic stem cell compartment. Trends Immunol. 2009; 30:360–365. [PubMed: 19540806]

Geiger H, Van Zant G. The aging of lympho-hematopoietic stem cells. Nat Immunol. 2002; 3:329–333. [PubMed: 11919569]

Greer EL, Maures TJ, Ucar D, Hauswirth AG, Mancini E, Lim JP, Benayoun BA, Shi Y, Brunet A. Transgenerational epigenetic inheritance of longevity in Caenorhabditis elegans. Nature. 2011; 479:365–371. [PubMed: 22012258]

Iden S, Collard JG. Crosstalk between small GTPases and polarity proteins in cell polarization. Nat Rev Mol Cell Biol. 2008; 9:846–859. [PubMed: 18946474]

Ito K, Hirao A, Arai F, Takubo K, Matsuoka S, Miyamoto K, Ohmura M, Naka K, Hosokawa K, Ikeda Y, et al. Reactive oxygen species act through p38 MAPK to limit the lifespan of hematopoietic stem cells. Nat Med. 2006; 12:446–451. [PubMed: 16565722]

Janzen V, Forkert R, Fleming HE, Saito Y, Waring MT, Dombkowski DM, Cheng T, DePinho RA, Sharpless NE, Scadden DT. Stem-cell ageing modified by the cyclin-dependent kinase inhibitor p16INK4a. Nature. 2006; 443:421–426. [PubMed: 16957735]

Ju Z, Jiang H, Jaworski M, Rathinam C, Gompf A, Klein C, Trumpp A, Rudolph KL. Telomere dysfunction induces environmental alterations limiting hematopoietic stem cell function and engraftment. Nat Med. 2007; 13:742–747. [PubMed: 17486088]

Kamminga LM, van Os R, Ausema A, Noach EJ, Weersing E, Dontje B, Vellenga E, de Haan G. Impaired hematopoietic stem cell functioning after serial transplantation and during normal aging. Stem Cells. 2005; 23:82–92. [PubMed: 15625125]

Karsunky H, Inlay MA, Serwold T, Bhattacharya D, Weissman IL. Flk2+ common lymphoid progenitors possess equivalent differentiation potential for the B and T lineages. Blood. 2008; 111:5562–5570. [PubMed: 18424665]

Kerber RA, O'Brien E, Cawthon RM. Gene expression profiles associated with aging and mortality in humans. Aging Cell. 2009; 8:239–250. [PubMed: 19245677]

Kiss TL, Sabry W, Lazarus HM, Lipton JH. Blood and marrow transplantation in elderly acute myeloid leukaemia patients - older certainly is not better. Bone Marrow Transplant. 2007; 40:405–416. [PubMed: 17572706]

Kohler A, Schmithorst V, Filippi MD, Ryan MA, Daria D, Gunzer M, Geiger H. Altered cellular dynamics and endosteal location of aged early hematopoietic progenitor cells revealed by time-lapse intravital imaging in long bones. Blood. 2009

Krishnan V, Chow MZ, Wang Z, Zhang L, Liu B, Liu X, Zhou Z. Histone H4 lysine 16 hypoacetylation is associated with defective DNA repair and premature senescence in Zmpste24-deficient mice. Proc Natl Acad Sci U S A. 2011; 108:12325–12330. [PubMed: 21746928]

Liang Y, Van Zant G, Szilvassy SJ. Effects of aging on the homing and engraftment of murine hematopoietic stem and progenitor cells. Blood. 2005; 106:1479–1487. [PubMed: 15827136]

Linton PJ, Dorshkind K. Age-related changes in lymphocyte development and function. Nat Immunol. 2004; 5:133–139. [PubMed: 14749784]

Ludford-Menting MJ, Oliaro J, Sacirbegovic F, Cheah ET, Pedersen N, Thomas SJ, Pasam A, Iazzolino R, Dow LE, Waterhouse NJ, et al. A network of PDZ-containing proteins regulates T cell polarity and morphology during migration and immunological synapse formation. Immunity. 2005; 22:737–748. [PubMed: 15963788]

Morrison SJ, Wandycz AM, Akashi K, Globerson A, Weissman IL. The aging of hematopoietic stem cells. Nat Med. 1996; 2:1011–1016. [PubMed: 8782459]

Peterson JR, Lebensohn AM, Pelish HE, Kirschner MW. Biochemical suppression of small-molecule inhibitors: a strategy to identify inhibitor targets and signaling pathway components. Chem Biol. 2006; 13:443–452. [PubMed: 16632257]

Pollina EA, Brunet A. Epigenetic regulation of aging stem cells. Oncogene. 2011

Rando TA. Stem cells, ageing and the quest for immortality. Nature. 2006; 441:1080–1086. [PubMed: 16810243]

Rando TA, Chang HY. Aging, rejuvenation, and epigenetic reprogramming: resetting the aging clock. Cell. 2012; 148:46–57. [PubMed: 22265401]

Rossi DJ, Bryder D, Zahn JM, Ahlenius H, Sonu R, Wagers AJ, Weissman IL. Cell intrinsic alterations underlie hematopoietic stem cell aging. Proc Natl Acad Sci U S A. 2005; 102:9194–9199. [PubMed: 15967997]

Rossi DJ, Jamieson CH, Weissman IL. Stems cells and the pathways to aging and cancer. Cell. 2008; 132:681–696. [PubMed: 18295583]

Rossi DJ, Seita J, Czechowicz A, Bhattacharya D, Bryder D, Weissman IL. Hematopoietic stem cell quiescence attenuates DNA damage response and permits DNA damage accumulation during aging. Cell Cycle. 2007; 6:2371–2376. [PubMed: 17700071]

Sakamori R, Das S, Yu S, Feng S, Stypulkowski E, Guan Y, Douard V, Tang W, Ferraris RP, Harada A, et al. Cdc42 and Rab8a are critical for intestinal stem cell division, survival, and differentiation in mice. J Clin Invest. 2012

Sengupta A, Duran A, Ishikawa E, Florian MC, Dunn S, Fickera A, Leitgese M, Geiger H, Diaz-Mecob M, Moscatb J, et al. aPKCζ and aPKCλ are dispensable for mammalian hematopoietic stem cell activity and blood formation. Proc Natl Acad Sci U S A. 2011

Signer RA, Montecino-Rodriguez E, Witte ON, McLaughlin J, Dorshkind K. Age-related defects in B lymphopoiesis underlie the myeloid dominance of adult leukemia. Blood. 2007; 110:1831–1839. [PubMed: 17554060]

Silva, H.; Conboy, IM. Aging and stem cell renewal. In: StemBook. , editor. The Stem Cell Research Community. 2008.

Sinha S, Yang W. Cellular signaling for activation of Rho GTPase Cdc42. Cell Signal. 2008; 20:1927–1934. [PubMed: 18558478]

Sudo K, Ema H, Morita Y, Nakauchi H. Age-associated characteristics of murine hematopoietic stem cells. J Exp Med. 2000; 192:1273–1280. [PubMed: 11067876]

Vaquero A, Sternglanz R, Reinberg D. NAD+-dependent deacetylation of H4 lysine 16 by class III HDACs. Oncogene. 2007; 26:5505–5520. [PubMed: 17694090]

Wang L, Yang L, Debidda M, Witte D, Zheng Y. Cdc42 GTPase-activating protein deficiency promotes genomic instability and premature aging-like phenotypes. Proc Natl Acad Sci U S A. 2007; 104:1248–1253. [PubMed: 17227869]

Xing Z, Ryan MA, Daria D, Nattamai KJ, Van Zant G, Wang L, Zheng Y, Geiger H. Increased hematopoietic stem cell mobilization in aged mice. Blood. 2006; 108:2190–2197. [PubMed: 16741255]

Yang L, Wang L, Kalfa TA, Cancelas JA, Shang X, Pushkaran S, Mo J, Williams DA, Zheng Y. Cdc42 critically regulates the balance between myelopoiesis and erythropoiesis. Blood. 2007; 110:3853–3861. [PubMed: 17702896]

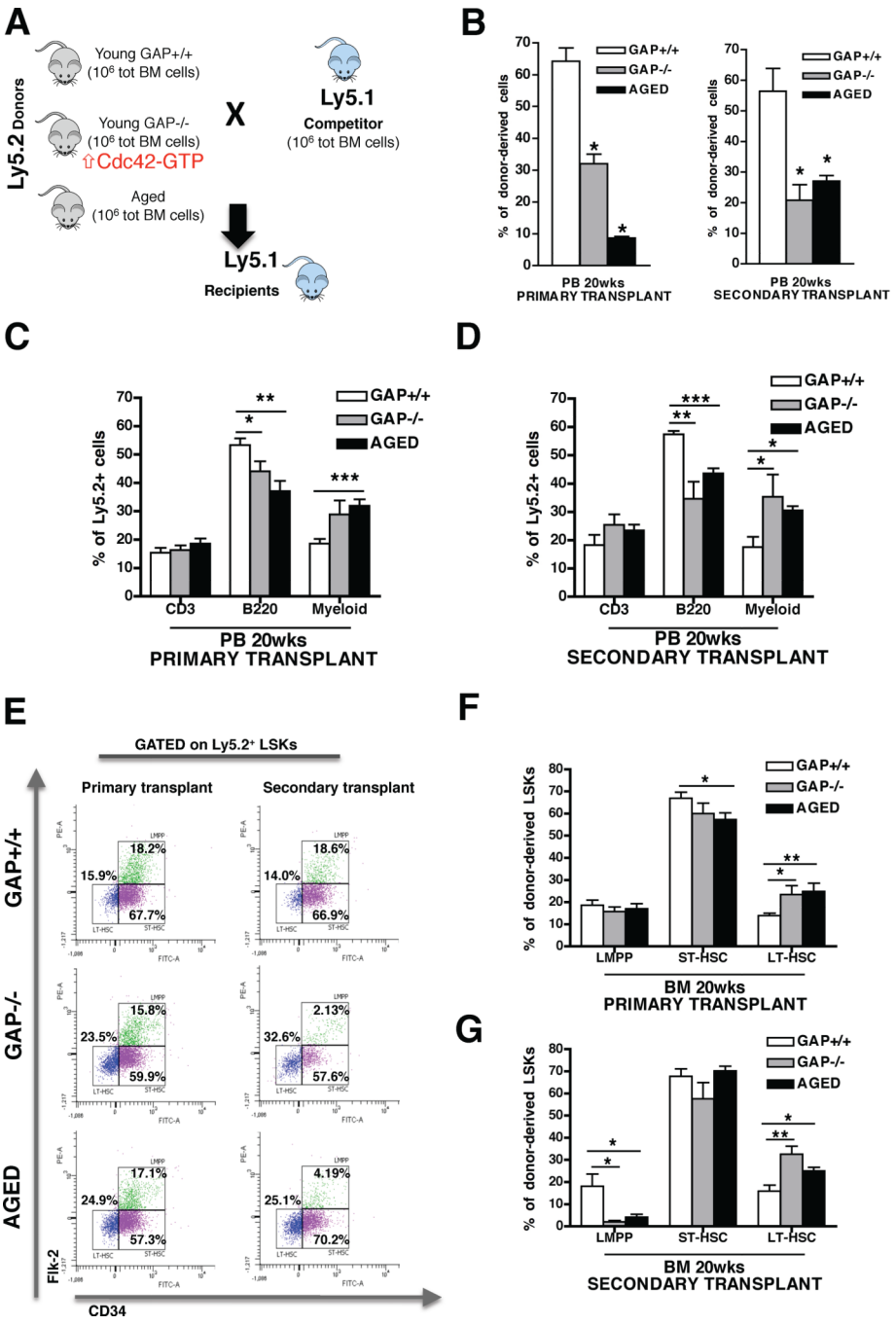

Figure 1. Constitutively increased Cdc42 activity results in premature aging of young HSCs

(A), Scheme of the experimental set-up for the competitive BM transplants. **(B)**, Contribution of total donor-derived Ly5.2$^+$ cells in PB after 20 weeks in competitive primary and secondary transplants. Percentages of engrafted cells are normalized according to stem cell equivalent. Mice were considered as engrafted when the percentage of Ly5.2$^+$ cells in PB was higher than 1.0 and contribution was detected for all PB lineages. **(C–D)**, Contribution of B-cells, T-cells and myeloid cells among donor-derived Ly5.2$^+$ cells in PB after 20 weeks in competitive primary (**C**) and secondary (**D**) transplants. (**E–G**), Representative FACS dot plots (**E**) and quantitative and statistical analysis of LT-HSCs, ST-

HSCs and LMPPs distribution among donor-derived LSKs in primary (**F**) and secondary (**G**) transplanted mice. * $P < 0.05$, ** $P < 0.01$, *** $P < 0.001$; columns are mean +1 S.E. The experiment was repeated three times with a cohort of 4 to 5 recipient mice per group (n = 14). See also Figure S1.

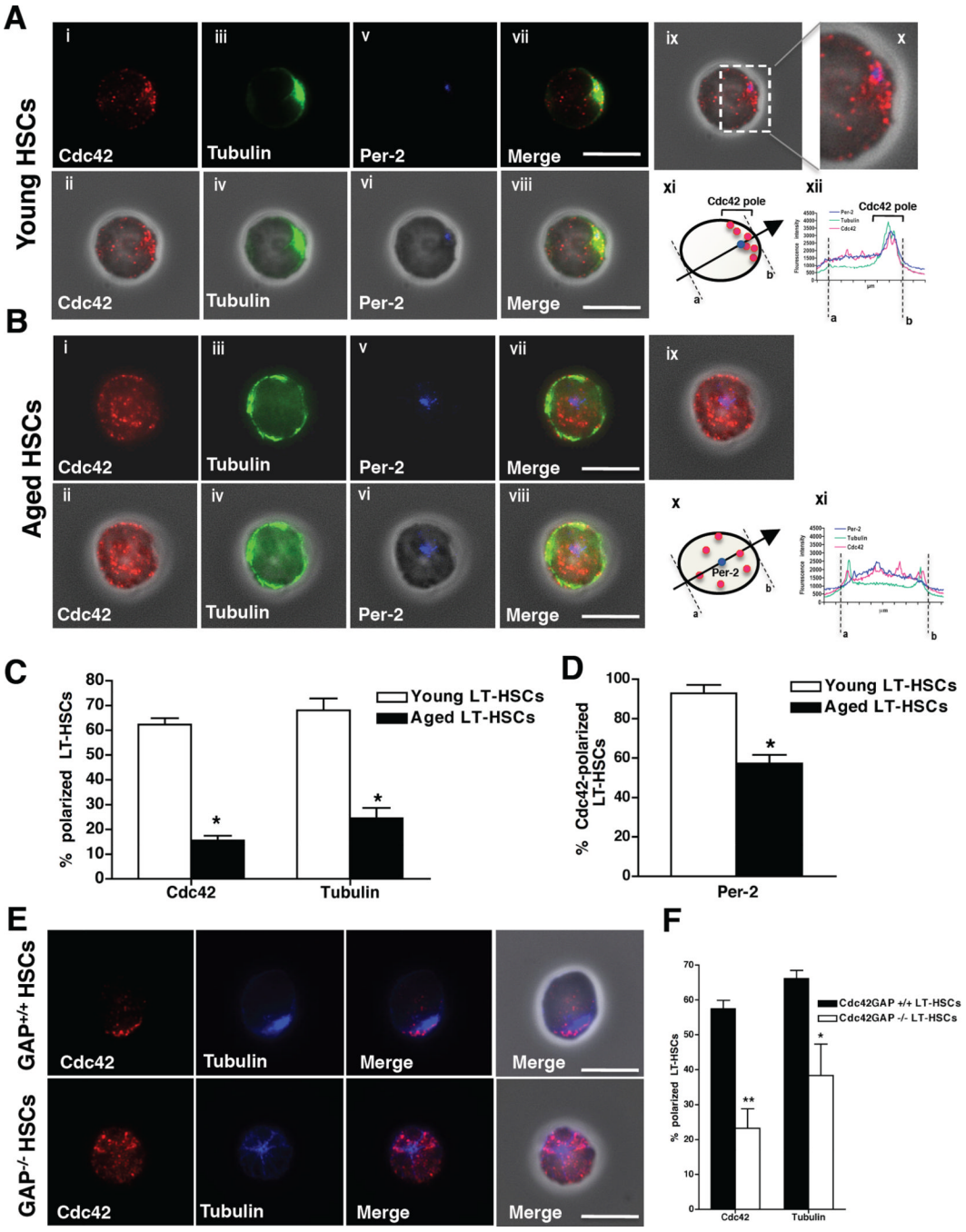

Figure 2. Increased Cdc42 activity correlates with a de-polarized phenotype in LT-HSCs

(A), Representative distribution of Cdc42, tubulin and pericentrin-2 (Per-2) in young LT-HSCs determined by IF. Pictures are shown on a dark background (panels i, iii, v and vii) or as overlap with the phase contrast picture (panels ii, iv, vi and viii). Bar = 5μm. Panel ix and x show Cdc42 (red) and Per-2 (blue) distribution over the phase contrast picture. Panel xi: schematic presentation of a representative distribution of Cdc42 in young LT-HSCs (Per-2, blue dot; Cdc42, red dots). The arrow indicates the direction from “a” to “b” followed for determining fluorescence intensity in panel xii. Panel xii: representative fluorescence intensity plot obtained by collecting pixel intensity through the section of the cell as

indicated in xi. **(B)**, Representative distribution of Cdc42, tubulin and Per-2 in aged LT-HSCs determined by IF. Pictures are shown on a dark background (panels i, iii, v and vii) or as overlap with the phase contrast picture (panels ii, iv, vi and viii). Bar = 5μm. Panel ix shows Cdc42 (red) and Per-2 (blue) distribution over the phase contrast picture. Panel x: schematic presentation of a representative distribution of Cdc42 in aged LT-HSCs (Per-2, blue dot; Cdc42, red dots). The arrow indicates the direction from "a" to "b" followed for determining fluorescence intensity in panel xi. Panel xii: representative fluorescence intensity plot obtained by collecting pixel intensity through the section of the cell as indicated in x. (**C**), Percentage of young and aged LT-HSC cells with a polar distribution of Cdc42 and tubulin. Shown are mean +1 S.E., n=10; ~500–700 cells scored per sample in total. * $p < 0.001$. **(D)**, Percentage of Per-2 polarized cells of Cdc42 polarized young and aged LT-HSCs. Cdc42-polarized cells were analyzed for Per-2 localization and scored positive when Per-2 was found at the Cdc42-pole. Shown are mean +1 S.E., n=4, ~150–250 cells scored per sample in total. * $p < 0.05$. **(E)**, Representative distribution of Cdc42 and tubulin in young Cdc42GAP$^{+/+}$ and Cdc42GAP$^{-/-}$ LT-HSCs. Pictures are shown on a dark background (panels i–vi) or as overlap with the phase contrast picture (panels vii and viii). Bar = 5μm. **(F)**, Percentages of young Cdc42GAP$^{+/+}$ (WT Control) and Cdc42GAP$^{-/-}$ LT-HSC cells with a polar distribution of Cdc42 and tubulin. Shown are mean mean +1 S.E., n=4, ~200–300 cells scored per sample in total. ** $P < 0.01$, *$P < 0.05$. See also Figure S2 and Movies S1–S3.

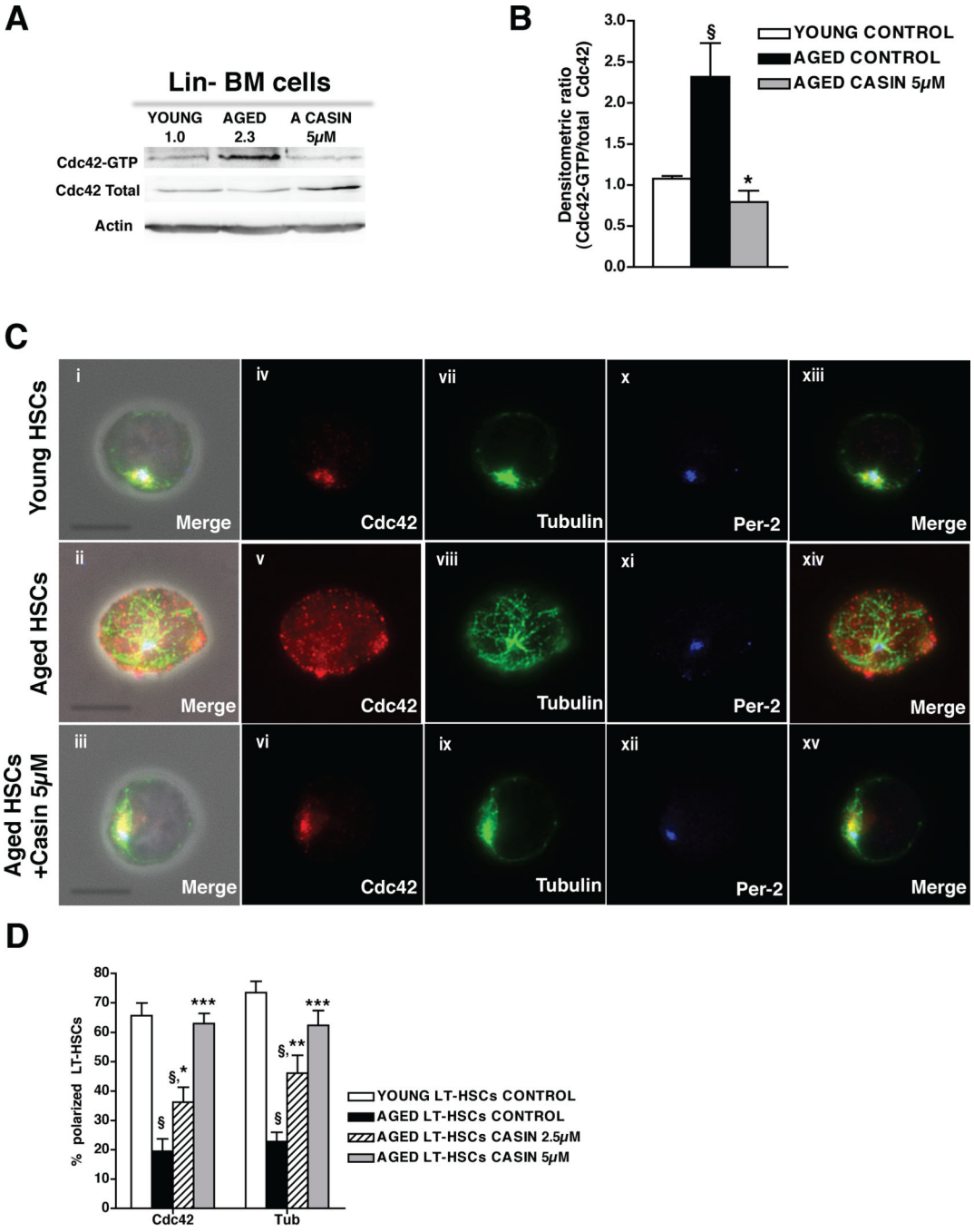

Figure 3. Pharmacological targeting of Cdc42 reverts aged apolar LT-HSCs to polar cells

(A), Representative Cdc42 activity in young, aged and CASIN (5 μM) treated aged lineage depleted bone marrow ($Lin^{-}BM$) as determined by a pulldown/Western Blot assay. Active Cdc42 (Cdc42-GTP) was normalized with respect to total Cdc42 and actin as delineated by the numbers. **(B)**, Ratio of the densitometric score of the Cdc42-GTP form and the total Cdc42 expression. Shown are mean +1 S.E., n=3, § $p < 0.05$ vs young control; *$p < 0.05$ vs. aged control. **(C)**, Representative distribution of Cdc42, tubulin and Per-2 in young, aged and aged LT-HSCs treated with 5μM CASIN. Shown are overlaps with the phase contrast picture (panels i–iii) or cells on a dark background (panels iv–xv). Bar = 5μm. **(D)**,

Percentages of cells polarized for Cdc42 and tubulin in young, aged and aged LT-HSCs treated with 2.5 and 5μM CASIN. For each sample cells were singularly analyzed and scored for Cdc42 and tubulin polar distribution. Shown are mean mean +1 S.E., n=4, ~200–300 cells scored per sample in total. § $p < 0.001$ vs young control; *** $p < 0.001$ vs. aged control, ** $p < 0.01$ vs. aged control, * $p < 0.05$ vs. aged control. See also Figure S3.

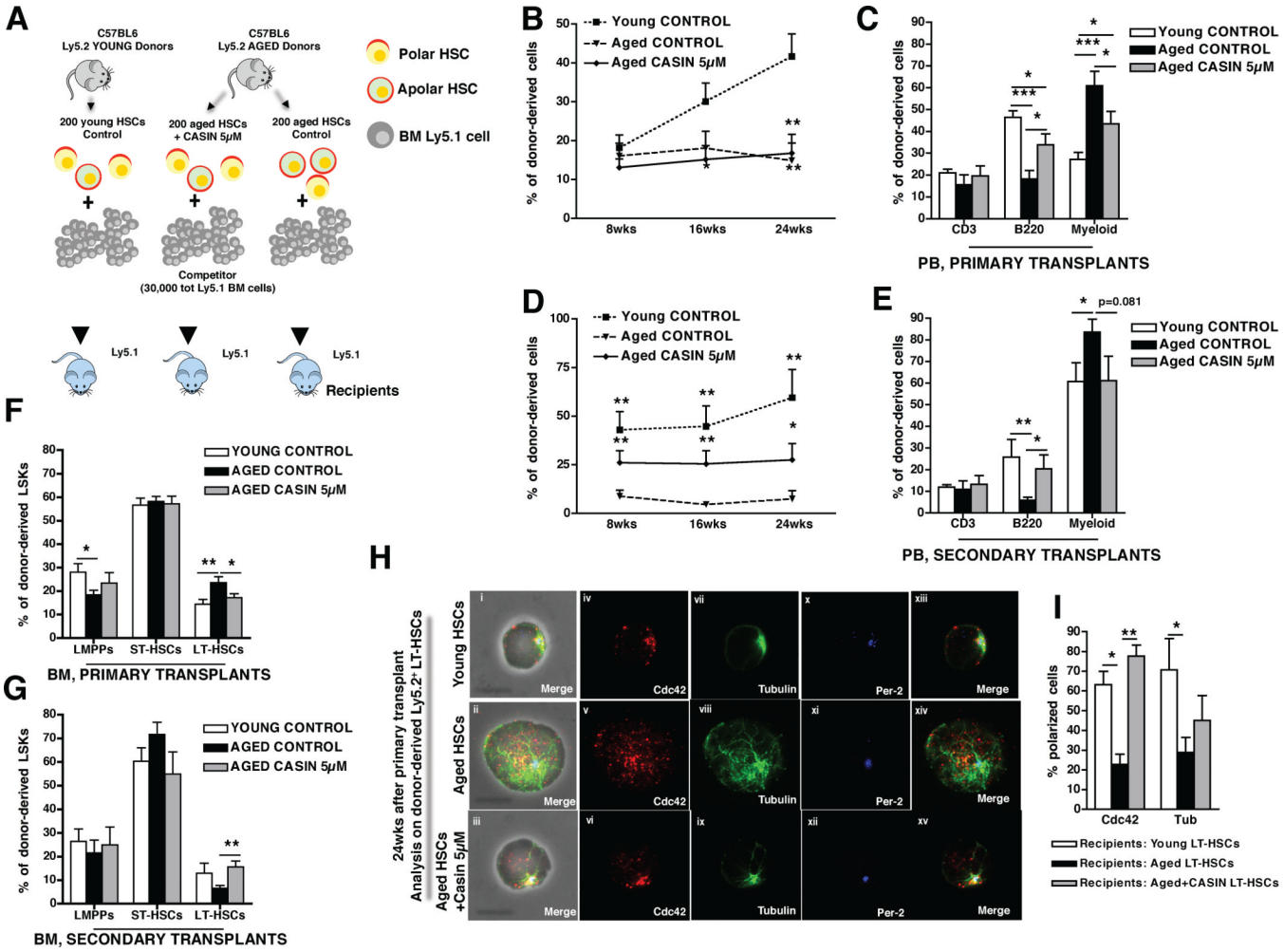

Figure 4. Pharmacological targeting of Cdc42 activity rejuvenates LT-HSCs function

(A), Schematic representation of the experimental setup. 200 aged and young donor ($Ly5.2^+$) LT-HSCs were cultured for 16hrs as indicated and subsequently transplanted into recipient ($Ly5.1^+$) mice along with 3–10^5 BM competitor ($Ly5.1^+$) cells. 24 wks post transplant recipient mice were sacrificed and secondary transplants were performed. **(B and D)**, Percentage of donor contribution ($Ly5.2^+$ cells) to total WBC in PB 8, 16 and 24 wks post transplant in primary (**B**) and secondary (**D**) transplants. Mice were considered as engrafted when the percentage of $Ly5.2^+$ cells in PB was higher than 1.0 in primary transplants and than 0.5 in secondary transplants and contribution was detected for all PB lineages. Shown are mean values +1 S.E.; ** $p < 0.01$ and * $p < 0.05$ vs young control in **B**; *** $p < 0.001$, ** $p < 0.01$, * $p < 0.05$ vs aged control in **D**. **(C and E)**, Percentage of $B220^+$, $CD3^+$ and myeloid cells among donor-derived $Ly5.2^+$ cells in PB 24 weeks after primary (**C**) and secondary (**E**) transplants. * $p < 0.05$, ** $p < 0.01$, *** $p < 0.001$; shown are mean values +1 S.E. **(F–G)**, Percentage of LT-HSCs, ST-HSCs and LMPPs cells in BM among donor-derived LSKs cells 24 weeks after primary (**F**) and secondary (**G**) transplants. ** $p < 0.01$; shown are mean values +1 S.E. Data is based on five (primary transplants) and four (secondary transplants) experimental repeats with 5 recipient mice per group (e.g. n=25 for primaries and n=20 for secondary transplants). **(H)**, Representative distribution of Cdc42, tubulin and Per-2 in donor-derived LT-HSCs sorted from young, aged and aged CASIN treated LT-HSC recipient mice 24 weeks post transplant. Shown are overlaps with

the phase contrast picture (panels i–iii) or cells on a dark background (panels iv–xv). Bar = 5μm. **(I)**, Percentage of donor-derived LT-HSCs polarized for Cdc42 and tubulin sorted 24 weeks post transplant from recipient animals competitively reconstituted with young, aged and aged CASIN treated LT-HSC. Shown are mean values +1 SEM, n=3, ~50 cells scored per sample in total. ** $p < 0.01$, * $p < 0.05$. See also Figure S4.

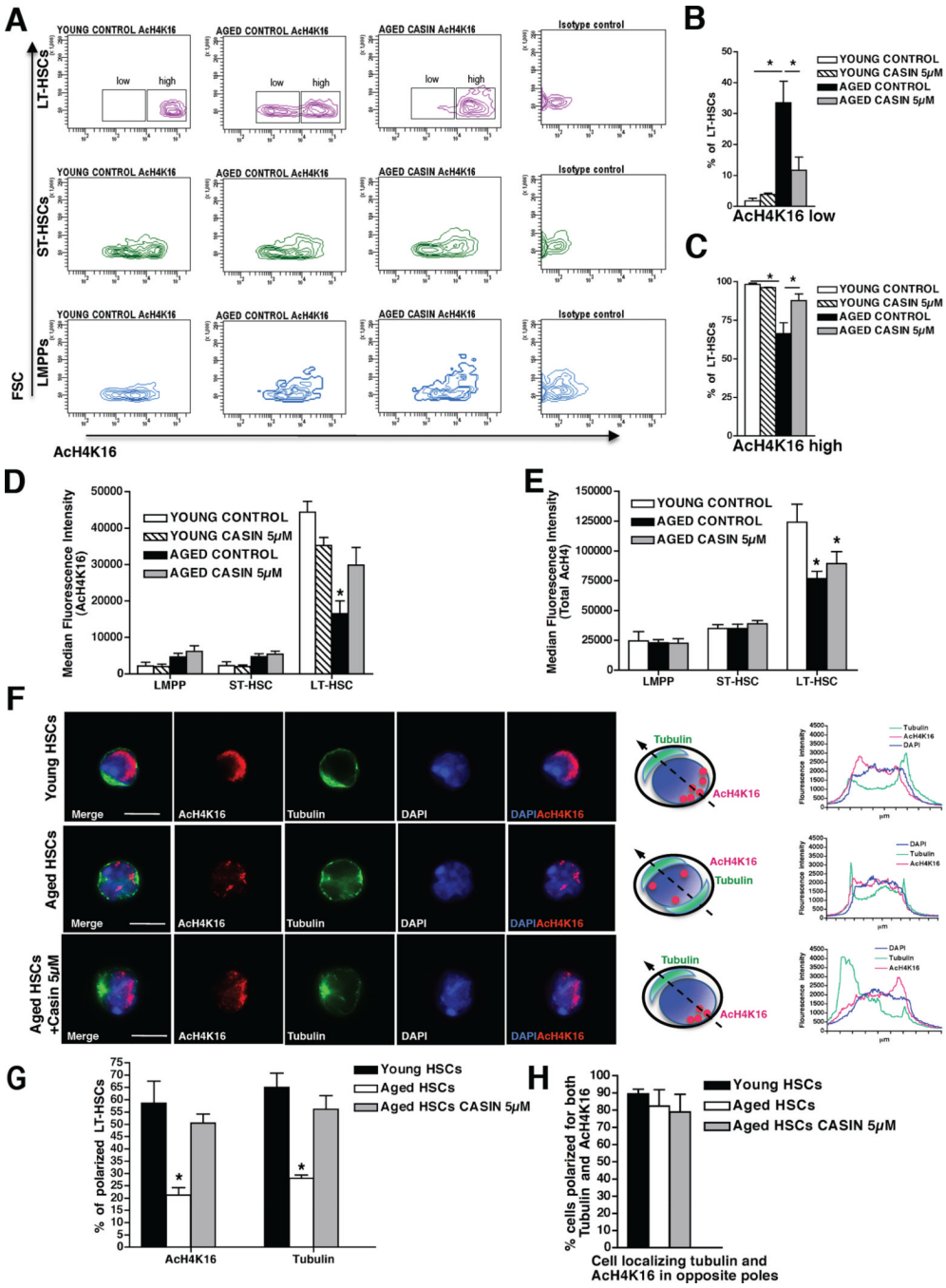

Figure 5. Pharmacological targeting of Cdc42 activity restores the level and the spatial distribution of histone H4 lysine 16 acetylation

(A), Representative FACS density plots of AcH4K16 expression in LT-HSCs, ST-HSCs and LMPPs. Aged LT-HSCs distribute in two distinct subpopulations expressing low and high AcH4K16 levels. **(B–C)**, Percentage of LT-HSCs expressing low **(B)** and high **(C)** levels of AcH4K16 according to the gating shown in **(A). (D–E)**, Median fluorescence intensity detected for AcH4K16 **(D)** and total AcH4 **(E)** in LT-HSCs, ST-HSCs and LMPPs. Shown are mean values +1 SEM, n=3. * $p < 0.05$. **(F)**, Representative distribution of AcH4K16 (red) and tubulin (green) in young, aged and aged LT-HSCs treated with 5μM CASIN. Nuclei are stained with DAPI (blue). Bar = 5μm. Schemes of Tubulin and AcH4K16

distributions in young, aged and aged LT-HSCs treated with 5μM CASIN and relative fluorescence intensity plot obtained by collecting pixel intensity through the section of the relative cell are also shown. **(G)**, Percentages of cells polarized for AcH4K16 and tubulin in young, aged and aged CASIN treated (5μM) LT-HSCs. For each sample cells were singularly analyzed and scored for AcH4K16 and tubulin polar distribution. The percentage of polarized cells is plotted over the total number of cells scored. **(H)**, Percentages of cells polarized for AcH4K16 and tubulin in opposite poles in young, aged and aged CASIN treated (5μM) LT-HSCs. The percentage of cells showing opposite polarity is plotted over the number of cells polarized for both markers. Shown are mean mean +1 S.E., n=3, ~100–150 cells scored per sample in total. * $p < 0.01$. See also Figure S5 and Movies S4–S5.